# A QUANTUM-MECHANICAL TIME-DEPENDENT SIMULATION OF THE SCATTERING FROM A STEPPED SURFACE

A.T. YINNON and R. KOSLOFF
*Department of Physical Chemistry and the Fritz Haber Research Center for Molecular Dynamics, The Hebrew University, Jerusalem, Israel 91904*

Received 12 August 1983

A recently developed time-dependent quantum-mechanical Fourier method is employed for the simulation of scattering atoms from surfaces of solids. The method allows exact calculation of scattering intensities, resonance strengths and lifetimes, in systems with a very large number of populated diffraction peaks. The study applies the method to the He/stepped copper surface. The accuracy of the method is checked by comparing to close coupling results for the He/W system.

## 1. Introduction

In recent years much experimental and theoretical effort has been focused on atom–surface scattering. Atom scattering has emerged as a standard probe in evaluating surface features. Theoretical effort has been devoted to constructing reliable simulations of the experiments. Simulations based on close coupling calculations have taken the lead in accurate quantum-mechanical calculations. On the other hand less accurate time-dependent classical trajectory studies have gained wide spread use. Their popularity is a consequence of ease of interpretation and implementation. It would seem therefore that time-dependent quantum-mechanical calculations should be able to bridge the gap between accuracy and ease of interpretation and could be used as a basis for simulations of actual experiments.

Pioneer work on quantum-mechanical time-dependent surface scattering was carried out by Raff [1], based on a finite difference code. This work suffers from unnatural boundary conditions and numerical dispersion of high-momentum states due to undersampling. In the present paper a Fourier method has been used which eliminates the difficulties of the finite difference method. The Fourier method implies periodic boundary conditions which are natural for surface scattering. The period of the grid is matched to the period of the unit cell. Due to the high accuracy of the method in calculating the kinetic energy operator numerical dispersion is eliminated. Numerical effort of the Fourier method grows slowly with the size of the problem. Therefore calculations are possible for systems which would include hundreds of channels if the close coupling method were to be used. Morever, the time-dependent method enables the direct calculation of resonance lifetimes. These advantages make the Fourier method especially suitable for the simulation of atom scattering from stepped surfaces, where the high corrugation means that there are many populated diffraction peaks. Hence until now scattering from stepped surfaces were performed by the classical trajectory method [2], the quantum-mechanical corrugated hard-wall method [3,4], and a convergent Born series [5].

In the present work the Fourier method is employed for the simulation of the He atoms scattered at low and high energy from the stepped Cu(117) surface. The method provides exact quantum-mechanical diffraction intensities for these systems, and the first direct resonance lifetimes calculation.

## 2. The Fourier method

The basis of the simulation of the scattering experiment is the time-dependent Schrödinger equation:

$$i\partial\psi/\partial t = H\psi, \tag{2.1}$$

0 009-2614/83/0000–0000/$ 03.00

where $H$ is the hamiltonian $H = P^2/2m + V$, and $\psi$ is the wavefunction. The numerical approximation is based on mapping the operators of the system into a discrete Hilbert space. The Fourier method represents the kinetic energy operator by transforming $\psi$ to $k$ space where the kinetic energy is diagonal, multiplying by $-k^2$ and transforming back to $q$ space. This transformation is brought about by a discrete Fourier transform. Numerical efficiency is achieved by the fast Fourier transform (FFT) algorithm, which means that the computing effort increases as $O(N \log N)$ where $N$ is the number of grid points.

Once the hamiltonian is represented, integration in time is achieved by explicit second-order differencing. More details on the Fourier method can be found elsewhere [6,7].

In order to construct the simulation, a few steps have to be followed. First the atom–surface potential has to be calculated on the grid points. The size of the grid is matched to the unit cell. The density of the grid, $dq$ is determined by the following constraints: $k_{\max} dq < \pi$, where $k_{\max}$ is the maximum momentum possible by conservation of energy. Since experimental studies of scattering of atoms in the direction of the steps have found no out of plane intensity [5], a two-dimensional simulation was sufficient, allowing for considerable saving in computation time.

Secondly the initial wave packet has to be generated. Two types of wave packets were used: localized and plane waves. Localized wave packets were constructed from gaussian waves in both $z$ direction (out of the surface) and the $x$ direction (perpendicular to the surface). The mean momentum in $x$, $k_x$, and $z$, $k_z$, was chosen in order to obtain the desired incident angle. Plane waves were constructed by utilizing the periodic boundaries in $x$. In $z$, a gaussian wave was still used. At this point the wave was propagated and at preselected time intervals analyzed. Analysis was done either in $q$ space or in $k$ space.

## 3. Application to the He/W system

In order to gain confidence in the new use of the Fourier method it was compared to a close coupling calculation for the He–W system. A two-dimensional repulsive Lennard-Jones–Devonshire potential was employed:

$$V(x,z) = D \exp(-2\alpha z)[1 - 2\beta \cos(g,x)], \tag{3.1}$$

the parameters of which are presented in table 1. The potential was cut at $V = 0.00089$ au in order to avoid small time integration steps. Also to save computation time the attractive part and a third dimension were excluded. The mean momentum in the $z$ direction was taken 3.43 au and in the $x$ direction 0 au. In order to allow for direct comparison of the diffraction intensities with the experiment (or with close coupling results), a plane wave in the $x$ direction and guassian wave in the $z$ direction with a width of 7 au were used. For such a large width, the energy spread of the wave is small. This means that the diffraction intensities for energies differing by the variance, calculated by the close coupling method, differ by less than 1%. If higher accuracy is demanded, an even larger width can be taken, requiring a larger grid in the $z$ direction.

The intensities of the diffraction peaks are presented in table 2 together with those calculated by the close coupling method (details about which can be found in ref. [8]). Since for normal incidence the population of the positive and negative diffraction peaks is equal, only those of the positive ones are presented. The dis-

Table 1
Parameters of the He/W system calculations. All parameters are given in atomic units

| | |
|---|---|
| He mass | 7344.4 |
| $D$ | 0.00012 |
| $\alpha$ | 0.582 |
| $a$ | 5.18 |
| $\beta$ | 0.01 |
| $nx$ | 32 |
| $nz$ | 32 |
| $dx$ | 0.97125 |
| $dz$ | 0.6 |

Table 2
Scattering intensities for He/W

| Peak | Fourier method | Close coupling method |
|---|---|---|
| 0 | 0.86104 | 0.86207 |
| 1 | 0.06906 | 0.06867 |
| 2 | 0.00041 | 0.00029 |

crepancy between the results of the two methods was less than 0.4%. This small discrepancy is due to the spread in the $k_z$ values.

## 4. Scattering from a stepped surface

For the simulation of atom scattering from a stepped metal surface, a one-dimensional stepped surface with flat terraces was assumed. Since for most metals the surface corrugation is very low and its effects on the scattering – in comparison with that of the steps – is small, this model was expected to reproduce the experimental results, i.e. intensities of diffraction peaks, multiple rainbows, and surface resonances.

The potential employed simulating the Cu(117) surface was of the following form:

$$V(x,z) = D\{\exp[-2\alpha(z - z_e)] - 2\exp[-\alpha(z - z_e)]\}, \tag{4.1}$$

where

$$z_e = z_0 + \tfrac{1}{2}\mathrm{SH}\cos[(x - x_2)\pi/(x_1 - x_2)] + \tfrac{1}{2}\mathrm{SH} + \mathrm{ns\,SH}, \tag{4.2}$$

where SH is the stepheight, $x_1 = \mathrm{ns\,SL} - \frac{1}{4}\mathrm{ad}$, $x_2 = \mathrm{ns\,SL} + \frac{1}{4}\mathrm{ad}$, ad is the atomic diameter, SL is the steplength, and ns is the number of steps from the origin to $x$. The parameters are presented in table 3.

Two simulations with flat waves in the $x$ direction and a width of 7 au in the $z$ direction were performed, with one for high mean momentum and one for low mean momentum. A third simulation was that of a localized wavepacket scattered in the vicinity of the step, providing insight into the details of scattering mechanism. (See also fig. 1.)

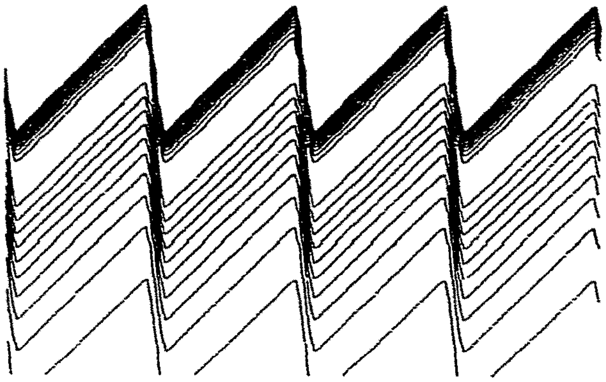

Fig. 1. Contour of stepped He/Cu potential. The $z$ direction is perpendicular to the surface, the $x$ direction is along the surface.

Table 3
Parameters of the He/Cu(117) calculations. All quantities are in atomic units

| | |
|---|---|
| He mass | 7344.14 |
| $D$ | 0.00012 |
| $\alpha$ | 0.6 |
| $a$ | 4.8378 |
| step height (SH) | 3.4208 |
| step length (SL) | 16.9323 |

### 4.1. Scattering of plane waves from stepped surfaces

The grid size, grid density, integration step, d$t$, mean momentum at high and low energies are presented in table 4. For scattering of a plane wave with $k_x > 0$, care should be taken to choose a value for $k_x$ such that the plane wave is periodic with the lattice, i.e. $k_x$ is an integer multiplication of $\pi/\mathrm{d}x$ gridsize.

The simulation at high energy, at which no resonance trapping occurred took ≈4 h of the VAX computer, whereas the computation time required for determining the different diffraction intensities in the low-energy case took 2 h. An additional 4 h were required for

Table 4
Grid parameters relevant to the scattering of a plane wave from Cu(117)

| | Mean momentum | |
|---|---|---|
| | $k_x = 0.510$<br>$k_z = 5.809$ | $k_x = 0.557$<br>$k_z = 1.926$ |
| $nx$ | 128 | 32 |
| $nz$ | 128 | 64 |
| d$x$ | 0.52913 | 1.05826 |
| d$z$ | 0.3 | 0.6 |
| d$t$ | 55.0 | 55.0 |

the determination of the lifetimes of the resonances. The mean lifetime of the adsorbed wave was $1.10 \times 10^5$ au.

The diffraction intensities and resonance strengths for both cases are presented in tables 5 and 6 respectively. For the high-energy case, the diffraction intensities calculated by the classical trajectory method are presented as well.

Table 5
Scattering intensities for He/Cu(stepped) for $E = 2.315 \times 10^{-3}$ au, $\vartheta_i = 5°$

| Peak | Fourier method | Classical trajectory method |
|---|---|---|
| 0 | 0.00878 | 0.00533 |
| 1 | 0.01569 | 0.00367 |
| 2 | 0.01908 | 0.00333 |
| 3 | 0.01816 | 0.00433 |
| 4 | 0.02202 | 0.00600 |
| 5 | 0.12815 | 0.01000 |
| 6 | 0.59323 | 0.71923 |
| 7 | 0.02494 | 0.04902 |
| 8 | 0.01021 | 0 |
| 9 | 0.00800 | 0 |
| 10 | 0.00452 | 0 |
| 11 | 0.00181 | 0 |
| 12 | 0.00084 | 0 |
| 13 | 0.00049 | 0 |
| 14 | 0.00040 | 0 |
| 15 | 0.00031 | 0 |
| −1 | 0.00107 | 0.00667 |
| −2 | 0.00544 | 0.00800 |
| −3 | 0.00660 | 0.00867 |
| −4 | 0.01059 | 0.00767 |
| −5 | 0.01567 | 0.00734 |
| −6 | 0.01616 | 0.00767 |
| −7 | 0.00945 | 0.00700 |
| −8 | 0.00439 | 0.00767 |
| −9 | 0.01016 | 0.00767 |
| −10 | 0.01161 | 0.00867 |
| −11 | 0.00312 | 0.01000 |
| −12 | 0.01454 | 0.01300 |
| −13 | 0.01709 | 0.01901 |
| −14 | 0.00300 | 0.02801 |
| −15 | 0.00327 | 0.02534 |
| −16 | 0.00139 | 0.01467 |
| −17 | 0.00068 | 0.00900 |

Table 6
Scattering intensities for He/Cu(stepped) for $E = 3.15 \times 10^{-4}$ au, $\vartheta_i = 5°$

| Peak | Diffraction intensities at time 143000 au | Resonance strength at time 396000 au |
|---|---|---|
| 0 | 0.00614 | 0.00013 |
| 1 | 0.01888 | 0.00011 |
| 2 | 0.81720 | 0.00007 |
| 3 | 0.01989 | 0.00091 |
| 4 | 0.02103 | 0.00533 |
| 5 | 0.00015 | 0.00010 |
| 6 | 0.00007 | 0 |
| 7 | 0.00007 | 0 |
| −1 | 0 | 0 |
| −2 | 0.00750 | 0.00016 |
| −3 | 0.00751 | 0.00024 |
| −4 | 0.01325 | 0.00037 |
| −5 | 0.02097 | 0.00187 |
| −6 | 0.01444 | 0.01071 |
| −7 | 0.02837 | 0.00915 |
| −8 | 0.00281 | 0.00008 |
| −9 | 0.00007 | 0 |

On viewing the results, attention should be paid to the following features: Both for the high- and low-energy case a multiple rainbow is distinguishable. This is in agreement with the experiment — the cause of which is explained in ref. [2]. For low energy, selective adsorption occurred: When the wave is examined as a function of time upon scattering, it is seen that a direct part if reflected from the surface followed by a slow leakage of the adsorbed part. The lifetime of the adsorbed part is extracted by examining the norm as a function of time. A first-order desorption process was obtained with a rate constant of $6.20 \times 10^{-6}$ au. In table 6 the diffraction intensities are represented for a time of 143000 au, where ≈13.7% of the wave is still adsorbed, and for the time of 360000 au, when only the adsorbed part is left.

Although there is no complete quantative agreement the classical and quantum-mechanical intensities, the classical trajectory method succesfully reproduces the position of the rainbow peaks. The percentage of the adsorbed atoms calculated by the classical method is 8.4%.

In figs. 2 and 3 plots are presented in respectively $q$

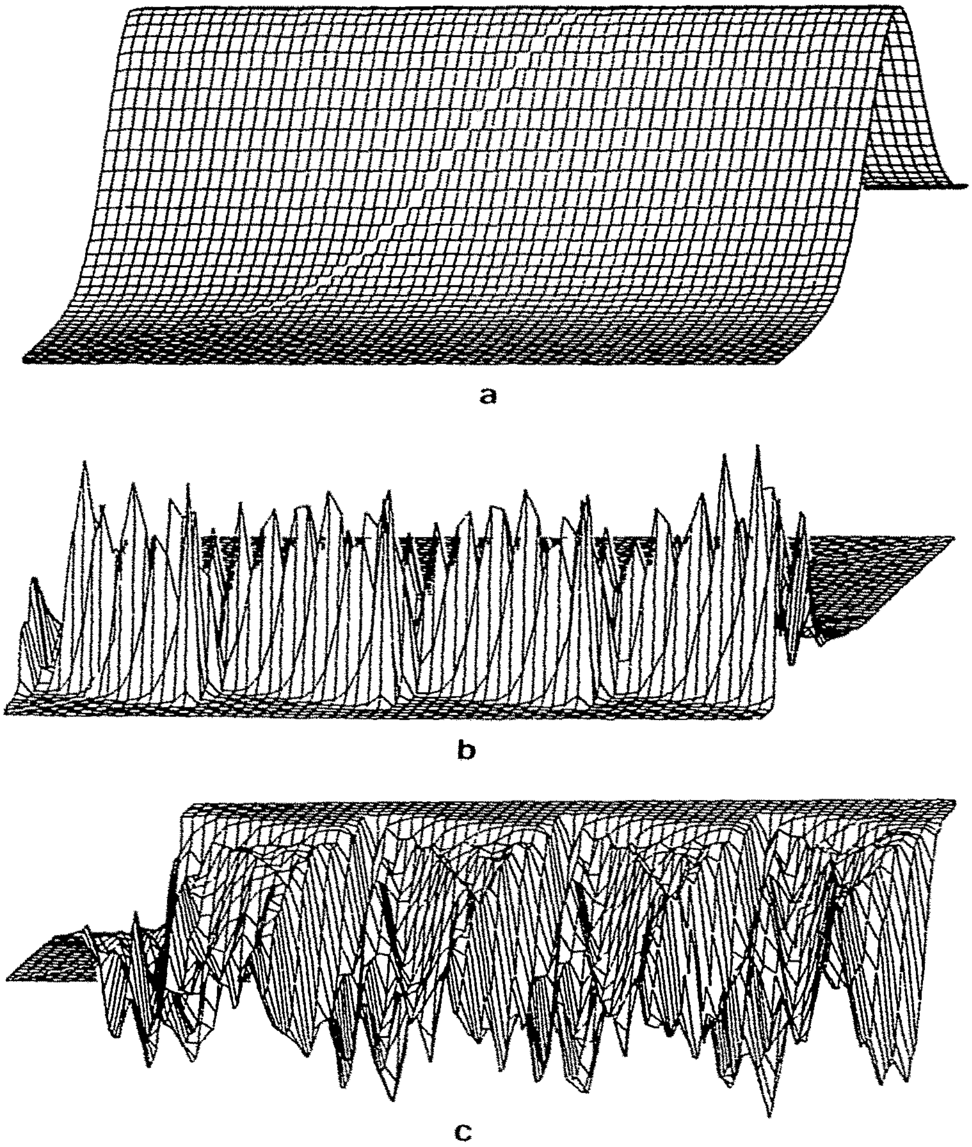

Fig. 2. Absolute value of the wavefunction in real space with $k_x = 0.557$ au, $k_z = 1.926$ au, (a) before it is scattered, (b) during the scattering process, (c) after it is totally scattered. $x$ direction is along the surface, $z$ direction is perpendicular to surface.

and in $k$ space of the wavefunction at different stages of the scattering process. The plane nature of the wave in the $x$ direction, and its large width in the $z$ direction are clearly distinguishable in fig. 2a, as well as its small dispersion in $k_z$ values (fig. 3a). Also significant in fig. 3c is the location of the diffraction peaks on a circle, a manifestation of conservation of energy in a region with constant potential.

### *4.2. Scattering of a wave packet from a step*

In this section the ability of the method to provide

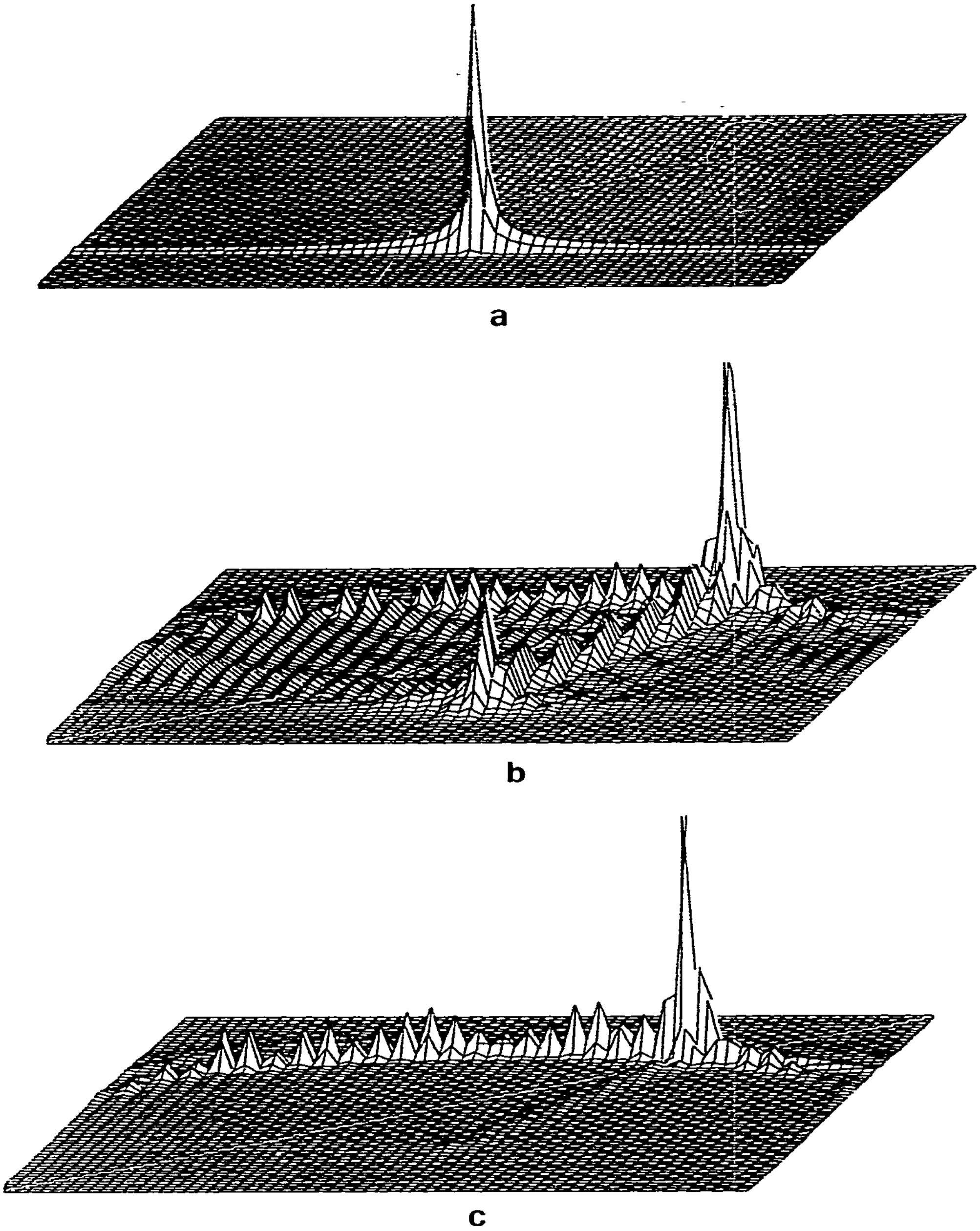

Fig. 3. Wavefunction in $k$ space with momentum as in fig. 2, (a) before it is scattered, the small ridge in $k_x$ is due to a boundary effect, (b) during the scattering process, (c) after it is totally scattered. The maximum $k_x$ and $k_z$ values are located at the borders of the grid. The positive $k_x$ values at the right of the grid and the negative at the left, the positive $k_z$ values at the top of the grid and the negative at the bottom of the grid.

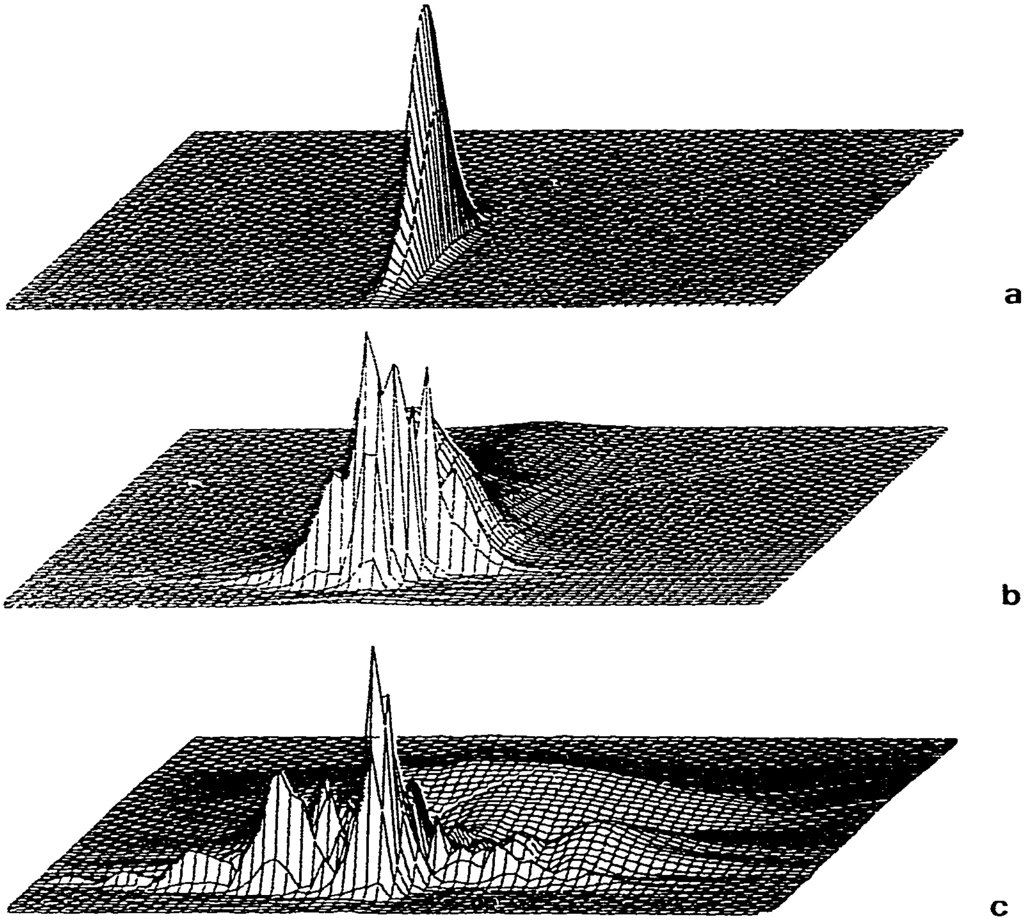

Fig. 4. Plots in real space of the collision of a wave packet with a step at different stages of the collision process (a) initial wave packet, (b) at the start of the collision, (c) near the end of the collision. The $x$ direction is along the surface, the $y$ direction is perpendicular to the surface. The apparent large width in the $z$ direction in comparison with that of the $x$ direction is due to the small grid density in the $z$ direction.

Table 7
Grid parameters of the scattering of a wave packet from a step. All quantities are in atomic units

| | |
|---|---|
| $k_x$ | 0.510 |
| $k_z$ | 5.809 |
| $wx$ | 4.0 |
| $wz$ | 4.0 |
| $nx$ | 128 |
| $nz$ | 128 |
| $dx$ | 0.52913 |
| $dz$ | 0.52 |
| $dt$ | 55.0 |

insight into the scattering process itself is demonstrated, a territory heretofore reserved for the classical trajectory method. A complete picture of the contributions of the different surface areas to the collision results can be obtained by scattering several wave packets with different impact parameters. Since the largest contribution to the formation of rainbows and resonances comes from scattering in the vicinity of the step, pictures of the wavefunction in real space at different stages of the collision are presented in fig. 4. The parameters concerning the grid and the wave packet are provided in table 7. The initial wave packet is presented in fig. 4a. In fig. 4b the scattering of the diffraction peaks are visible, whereas in fig. 4c the influence of the step on the population of the high-order diffraction peaks, is noticed.

## 5. Summary and conclusions

Two main features of the Fourier method emerge from this work. First the ability to simulate atom surface collisions accurately. The slow growth of computation time with the number of channels means that simulations are possible for extremely corrugated surfaces. The second feature is the ability to follow in time the progression of the collision. Much insight can be gained from plots of the wavepacket at different times. Moreover the method enables a time scale separation of scattering phenomena. In this fashion the direct and adsorbed parts of the low-energy surface collision were separated, and the mean lifetime of the adsorbed part calculated. Another feature of the time-dependent Fourier method not exploited in this work is the inclusion of phonons. However their inclusion into the model is possible by employing a Langevin potential [9]. Work on these lines is in progress [10].

Since the method calculates the wavefunction in continuous *k* space, it allows for the exact quantum-mechanical computation of a wavefunction (atom) scattered from a surface with adsorbed impurities or from disordered surfaces. Further work on these subjects is in progress.

## Acknowledgement

Work supported by the Israel Academy of Science and Humanities. The Fritz Haber Research Center is supported by the Minerva Gesellschaft für die Forschung, GmbH, Munich, FRG.

## References

[1] P.M. Agrawal and L.M. Raff, J. Chem. Phys. 77 (1982) 3946.
[2] A.T. Yinnon, U. Minlegrin and R.B. Gerber, J. Chem. Phys. 73 (1980) 5363.
[3] J. Harris, A. Liebsch, G. Comsa, G. Mechtersheimer, B. Poelsma and S. Tomoda, Surface Sci. 118 (1982) 279.
[4] J.G. Mantovani and J.R. Manson, Surface Sci. 120 (1982) L 487.
[5] A.G. Armand, J. Lapujoulade, J.R. Manson, J. Perreau and B. Salanon, Israel J. Chem. 22 (1982) 298;
B.J. Perreau and J. Lapujoulade, Surface Sci. 119 (1982) L292.
[6] D. Kosloff and R. Kosloff, J. Comput. Phys. (1983), to be published.
[7] R. Kosloff and D. Kosloff, J. Chem. Phys. (1983), to be published.
[8] A.T. Yinnon, S. Bosanac, R.B. Gerber and J.N. Murrell, Chem. Phys. Letters 58 (1978) 364.
[9] S.A. Adelman and J.D. Doll, J. Chem. Phys. 61 (1974) 4242;
S.A. Adelman, Advan. Chem. Phys. 44 (1980) 143.
[10] R. Kossloff and C. Cerjan, to be published.